Original Research Paper

IJES *Iranian Journal of Earth Sciences*
Vol. 14, No. 3, 2022, 178-185.
DOI: 10.30495/IJES.2022.1933137.1624

Resistivity surveys application for detection of shallow caves in a case example from Western Iraq

Ali Mishaal Abed*[1], Kamal Kareem Ali[1], Asama Hamud Al-Jumaily[1]

1. Department of Applied Geology, College of Science, Anbar University, Ramadi, Iraq.

Received 23 July 2021; accepted 29 October 2021

Abstract

The 2-D and 3-D imaging resistivity techniques were used in the current study to determine the shallow subsurface caves in the Haditha region, western Iraq. The 2-D resistivity imaging has been applied at five locations. The dipole-dipole arrangement was selected with an electrode spacing of 2 m. The inverted models show the anomalous resistivity variation between the background rocks and the voids. Which showed shallow cavities at 1 to 6 m depth, whereas some of them are extending to a depth of 23 m. The unconformity layer between Anah and Euphrates formations is the lowest cohesive than the rocks beneath and above it. Providing the best area for the caves to be formed resulted from dissolving its rocks by leaking rainwater and groundwater. The 3-D resistivity imaging technique was selected near some visible caves by collating seven 2D imaging lines in mapping the subsurface extent of such cavities. 3D imaging draws a sub-surface image in presence of 3D inhomogeneity such as caves. The horizontal slices of 3D models show up these caves with anomalous high resistivity at 0-0.80 m, 0.80-1.72 m, 1.72-2.78 m, and 2.78-3.99 m depths. It also shows a group of small caves, such as the sink-hole canals that connect the main cave to the surface. Both 2-D and 3-D resistivity models have marked a very similar spread of subsurface caves in the study area and show some caves, in the upper part of the unconformity layer. The large values of RMS error for models, attributed to the presence of large homogeneities in the study area. Such heterogeneities are mainly caused by a large variation in the subsurface resistivity of the rocks surrounding the caves and the large spread of shallow caves.

Keywords: *2-D and 3-D imaging technique, Dipole-dipole array, cavity, Haditha, Iraq.*

1. Introduction

The Haditha region characterizes by the presence of many caves visible within the rocky outcrops. Some caves were observed to have 5 m height (Fig 1). In addition, many small openings are connected to the sub-surface caves. In the study area, there is also an opening of a cave approximately three meters wide, formed as a result of a bulldozer's work to level the ground for the construction of a primary school. The foregoing indicates that the study area represents a risk area. Therefore, it was necessary to conduct an electrical survey to inspect the subsurface caves to help the concerned authorities to make a suitable decision when constructing buildings in the area. Cavities in carbonate rocks within the basal breccia unconformity layer between Anah and Euphrates formations have been formed as a result of dissolving rocks by water-rock interaction (Sissakian et al. 2005). They cause severe troubles for civil engineering and environmental management. The main type is sinkholes, which have been developed in various shapes and dimensions (Bentley and Gharibi 2004). Canals and voids would develop by infiltration of the groundwater through weak areas of limestone (Elawadi et al. 2001). Resistivity surveys such as 1-D, 2-D, and 3-D imaging used in the determination of subsurface cavities, voids, and features of weak areas, by several researchers such as (Dutta et al. 1970; McDowell 1979; Al-Ane 1993; Al-Zoubi et al.2007; Massoud et al. 2009; Yilmaz 2011; Obiadi et al. 2012; Abed 2013; Salman et al. 2020 a; Salman et al. 2020 b; Abed et al.2020;).

3-D resistivity imaging surveys are widely used in geophysical explorations as they reveal highly convoluted geological structures in three-dimension (Dahlin and Loke 1997; Dahlin et al. 2002; Bentley and Gharibi 2004). This is because the 2-D imaging Requires high costs of large enough area as compared to other areas. Full 3D resistivity imaging using the 3-D interpretation technique gives, in theory, the most accurate results (Bentley and Gharibi 2004). The 3-D resistivity imaging was collected by arranging the electrodes in the form of multiple 2-D profiles, so the apparent resistivity was calculated in all directions. (Chambers et al. 2006; Chambers et al. 2012). This technique reveals highly convoluted geological structures in three-dimension in the current study.

To create models with Dipole-dipole array in Hit area, west to the current study area, Abed et al. (2021) employed two 2D and 3D inversion methods: least squares and robust constrain inversions. They were able to locate the cave, but the second was more precise because the cave's dimensions in the inverse model are very close to the actual dimensions. The horizontal slices served as the basis for the final 3D model, which was used to find a 3D impedance distribution at depth. After 1.5 m on the model slices, the effect of the Um El-Adam cavity shows, which is represented by an increase in resistivity contrast compared to the surrounding

*Corresponding author.
E-mail address (es): sc.amah_mishal@uoanbar.edu.iq

formation. The size of the cavity was discovered to be larger than the real measurements at 3-4 m depth. Al-Hetty et al. (2021) concentrated their research on two key sites in the west of Al Anbar Governorate that have numerous caves. The first location is the Um El-Githoaa hollow within gypsum rocks in the Hit region's Fatha Formation (middle Miocene). The cave is located in an unconformity breccia zone between the Anah Formation (Upper Oligocene- Lower Miocene) and the Euphrates Formation (Lower Miocene- Middle Miocene), which stretches along the boundary between the Anah and the Euphrates Formations, leading to its extension for large distances.

The gypsum caves, on the other hand, were found to This method is more cost-effective which treats each two-dimensional line separately to allow making quality control (Rucker et al. 2009). The second technique is to collect data as a set of individual 2D lines (X or Y), Followed by the process of building a 3-D reflection to create a 3D model by integrating these lines into 3-D data. Therefore, the distances between the 2D lines and the type of electrode array used to have a great influence on the accuracy of 3-D imaging (Dahlin and Loke 1997; Yang and Lagmanson 2006; Aizebeokhai and Oyeyemi 2014; Loke 2020). Three-dimensional field techniques are widely used by many researchers, as their results are satisfactory for accuracy and clarity (Loke and Barker 1996; White et al. 2001; Dahlinet al. 2002). The primary goal of this research is to determine the extent of shallow voids beneath the breccia unconformity layer between the Aanah and Euphrates formations that are expected to be near the ground surface.

2. Materials and methods

2.1. Description site and stratigraphy

The research location is in western Iraq, south of Haditha city. It's between 34° 00' 6.11" and 34° 00' 24" north latitude and 42° 20' 12.45" and 42° 20' 46.11" east longitude (Fig 2).

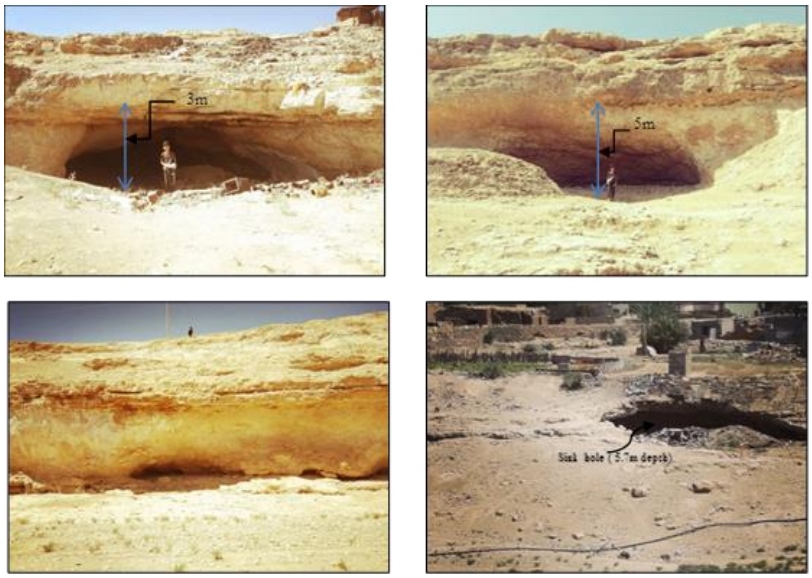

Fig 1. Photographs of cavities in Haditha city, western Irag

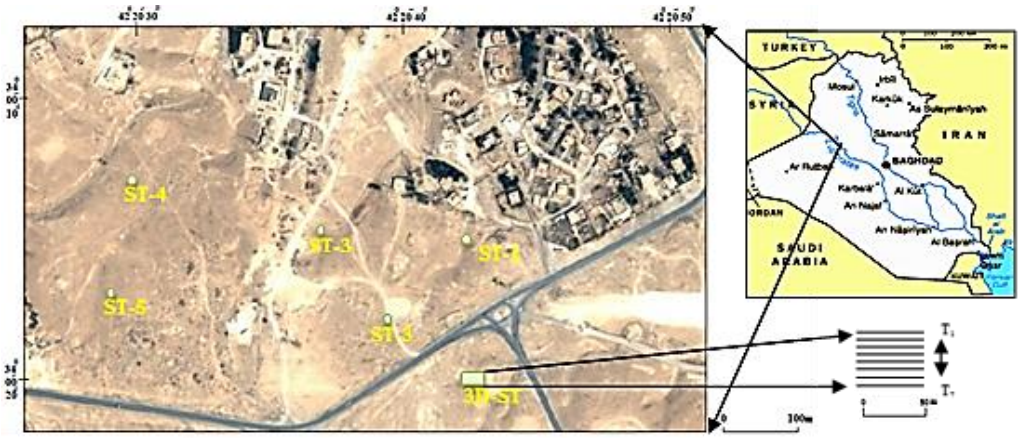

Fig 2. Location of study area

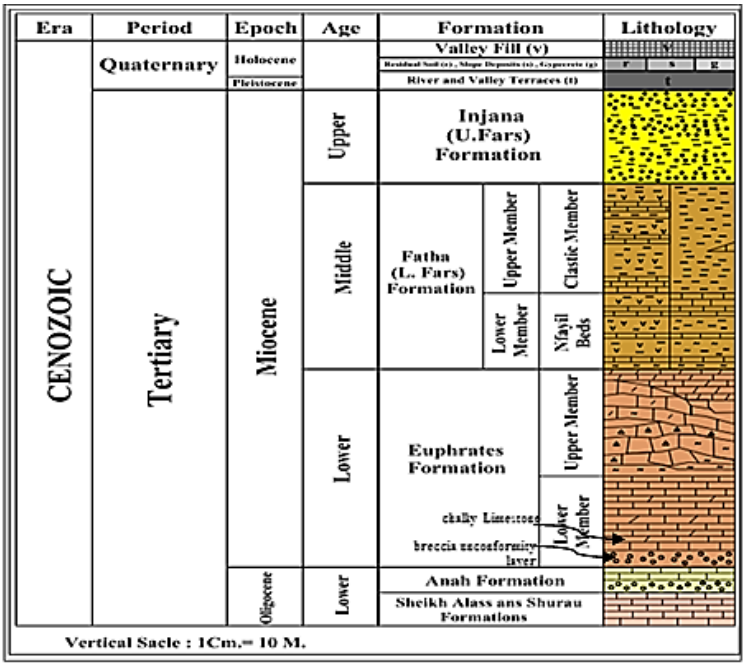

Fig 3. The stratified sequence of geological formation in the Haditha area (Sissakian and Salih 1994)

The study region is made up of sedimentary strata dating from the lower Oligocene (Shurau and Sheikh Alas formations) to upper Oligocene-Miocene (Anah and Euphrates formations), covered with different types of Quaternary deposits (Pleistocene-Holocene). (Sissakian and Salih 1994) (Fig 3).

2.2. Data acquisition

In this study, the ABEM Terrameter SAS 4000 was used. The 2-D survey measurements were taken at five different locations. (ST-1 to ST-5 in Fig 2). The dipole-dipole array was carried out using an a-electrode spacing of 2 m. A survey line of 42 electrodes at stations ST1 and ST5 and 22 electrodes at stations ST2, ST3, and ST4 was used to design the forward sequence of apparent resistivity (a) measurements. The 2-D stations were selected within the planned areas of new civilian facilities added to the Urban planning of the study area. At 3D-Station, to create a 3-D model of shallow subsurface cavities, the 2-D imaging data were set off seven traverses T1 to T7 (Each Traverse includes 42 electrodes, Dipole-dipole array applied in the measurement process for resistivity and with an electrode spacing of 2m and profile spacing of 4 m in one data file as a text to obtain 3-D models by using the RES3DINV program and to be used later for inversion processes.

3. Results and discussions

3.1. 2-D data interpretation

RES2DINV ver. 4.9.15 (Geotomo Software, 2019) interpret 2D resistivity imaging data using standard least squares and robust constrain inversion models. The standard data least squares method is used to produce a model with gradient boundaries in clarity due to layers. The Robust constraints inversion model was also used, to characterize the sharp borders for cavities, voids, and fractures (Busby 2000; Loke 2020).

The first station (ST-1) is located on the eastern side of the study area. The inverted model (Fig 4) reveals the presence of the main cave, which begins at a depth of 3 meters and extends to a depth of 23 meters in the middle of the trail. There are also several small caves to the right and left of the main cave, some of which have leaky groundwater, which has low resistivity values (Fig 4). The cavity wall has a gradational boundary in this model, which was created using the normal least-squares method. The model created by the robust model inversion method (Fig 5) has sharp and regular boundaries in contrast. So, the least-square inversion method is used in the interpretation of the other 2-D resistivity data because the cavity shape is irregular.

At station 2, the inverse model of 2-D data produced by the standard least-squares method has a gradational boundary for the cavity wall. This model indicates the existence of a large cave with a length equal to thirty determined because it extends to depth more than the investigated section. The lower part of the cave is distinguished by its low resistivity, so we expect that there will be water in this part (Fig 4).

The third station is in the center of the research area. The major cave, which runs from the center of the traverse to the south of the study area, was discovered. Due to its emptiness, the cave has high resistivity values

in the range of 7 ohm.m. It is around 5 meters below the earth's surface. It is surrounded from the top by several small caves. The fourth station is located in the west of the study area. Figure 4 shows the presence of two caves in the middle of the path and west of the study area, at a depth of about 3 and 1 meters, respectively. These caves are characterized by relatively high resistivity values between 400 and 500 ohms. The fifth station is characterized by some small caves spread near the surface of the earth. So the southern part of the study area has more risks for the buildings.

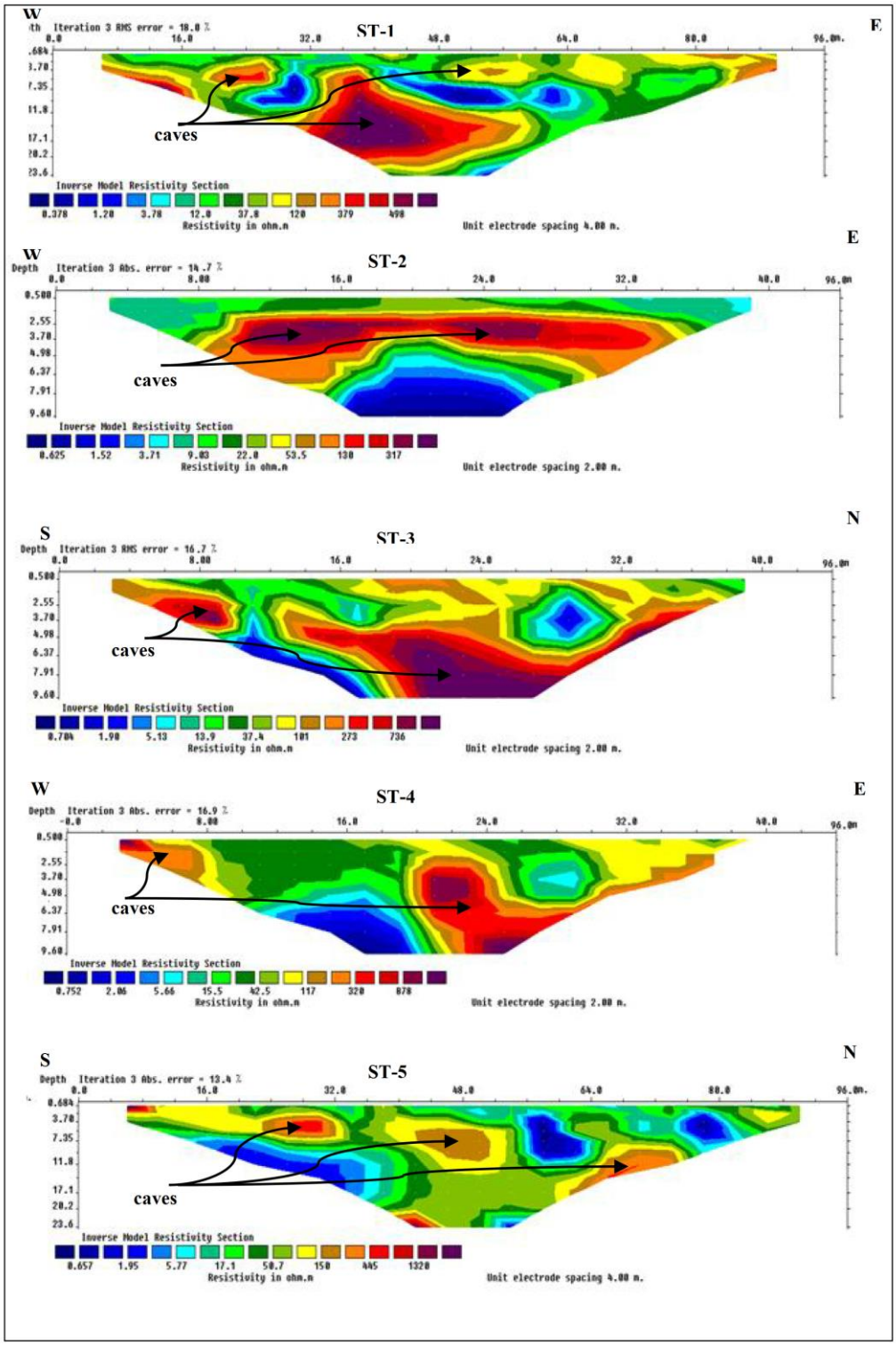

Fig 4. Dipole-dipole 2D resistivity Inverse mode (Standard least-squares option).

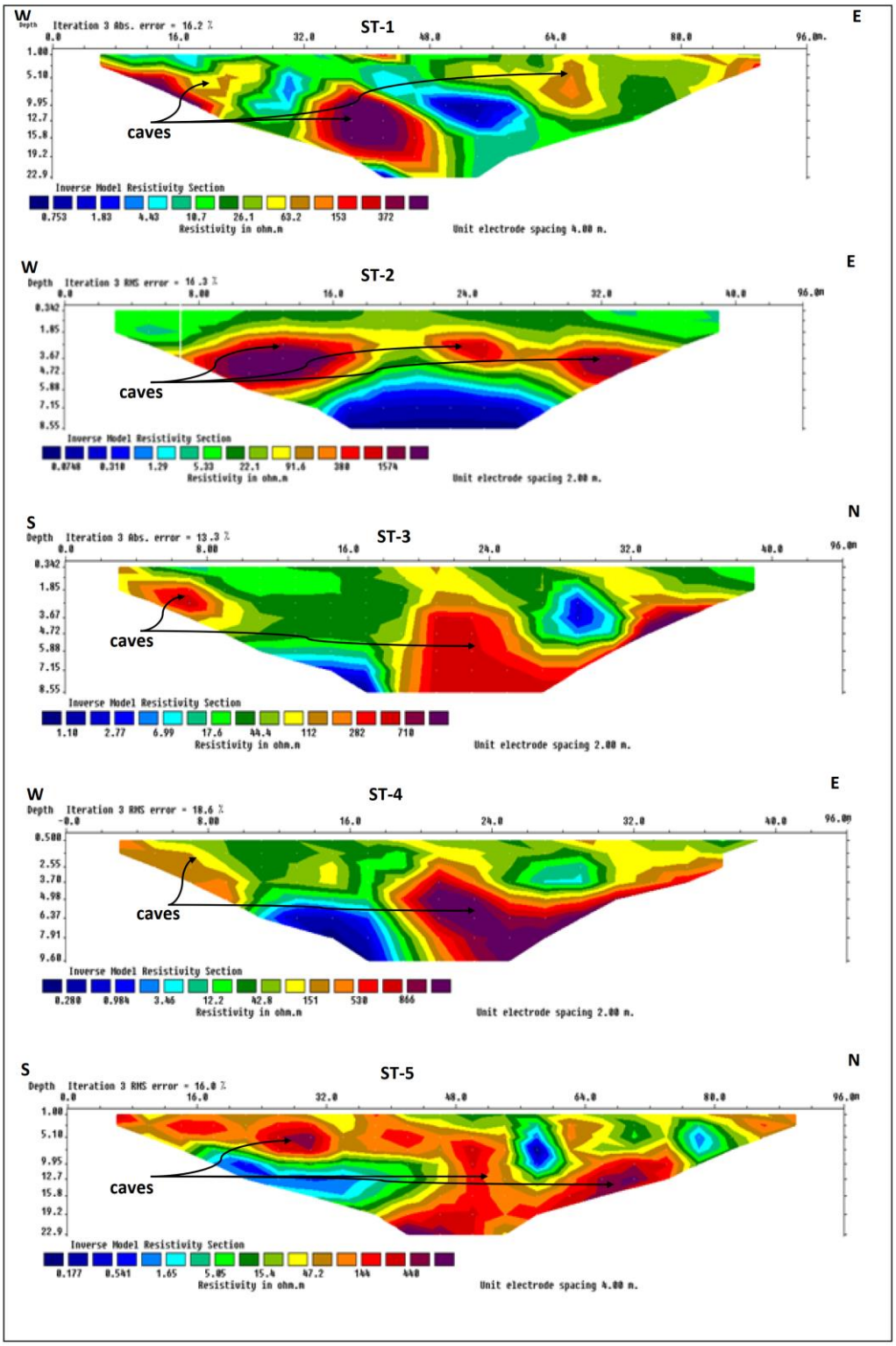

Fig 5. Dipole-dipole 2D resistivity Inverse mode (Robust inversion model option)

3.2. 3-D data interpretation

For a limited area within the research area, a 3-D resistivity display of the underlying structural geology was created (using seven 2D parallel profiles). All profiles are arranged in a single data file that was read with the RES3DINVsoftware to be and inverted to obtain the 3D model. RES3DINV software (Geotomo Software, 2019) is a computer program designed to generate a 3D resistivity model from the observed data

(White et al. 2001; Li and Oldenburg 1992). In this study, it was used to produce 3D inverted models.

The program's inversion routine is based on the smoothly constrained least-squares method (Sauck, 1998). It is also possible to utilize a new application of the least-squares method based on Newton's quasi-refinement methodology (Loke and Barker 1996; Loke and Dahlin 2010). This technique can be 10 times faster than the traditional least-square method for large data sets and requires less memory.

We can use the technique that can directly apply a ductility limit to typical resistivity values. On the other side, the Robust option is also available that tends to have a sharp border in anomalies patterns. The inversion program divides model space into many small rectangular blocks and attempts to determine the resistivity values of the blocks to iteratively reduce the difference between the resistivity values calculated and observed.

The optimization method is used to minimize the difference between the calculated and measured apparent resistivity values as an attempt to adjust the resistivity of the model blocks. This difference gave by measuring the root-mean-squared (RMS) error. In general, the more realistic approach is to select the model of iteration after which the RMS error does not change significantly. Inversion results can be displayed as slices of varying depths in the program. Every slice is a representation of the real resistivity distribution at the depth chosen. Figure (6) shows a well 3-D resistivity distribution in the x and y direction with z-direction (depth). slices between 0-2 m show the significant resistivity variation, with relatively high values due to dry sediments. Inversion findings can be shown as slices of varying depths by the application. Each slice is a map of the real resistivity distribution at the depth selected.

These caves are clearly shown as points with highly variable resistivity values in slices of depths 0-0.80 m, 0.80-1.72 m, 1.72-2.78 m, and 2.78-3.99 m, which reflect the heterogeneity between the rock components in this zone.

At a depth of 4.72 to 6.13 meters, a group of small caves appears, such as the sink-hole canals that connect the main cave to the surface but in some cases, this is not true at a depth of about 4 m. Especially if there is a high amount of geological noises near-surface, and the noise is usually more common with the dipole-dipole array that has a very large geometric factor, and thus very small reading between a potential electrode (Loke 2020). The cavity is located in the middle of the study area, and the bottom of the cave disappears at a depth of 14 meters. Figure 6 and Figure 7 show the comparison between standard least-square and the robust constrain methods. The second method shows that the inverse model produced has sharper and straighter boundaries.

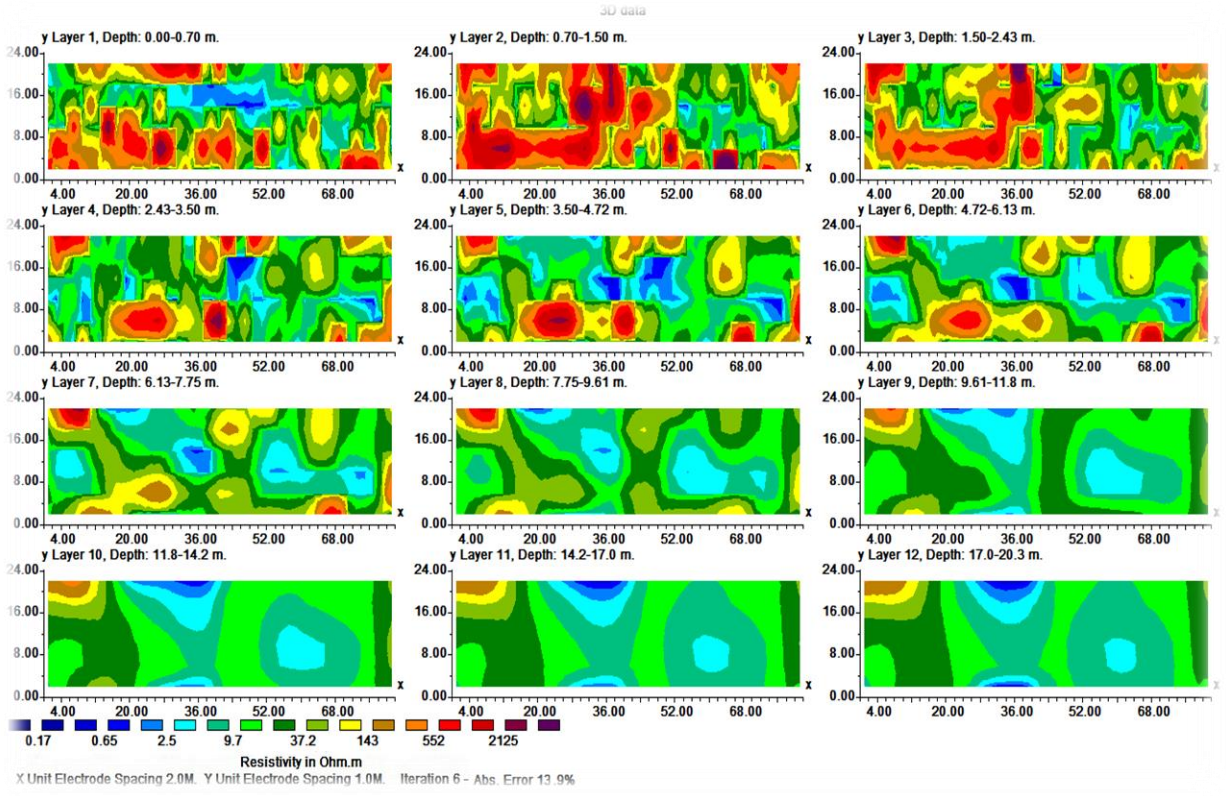

Fig 6. Inversion model for shallow unknown cavities shows 3-D resistivity distribution level slices for different depths using the standard Least-square method

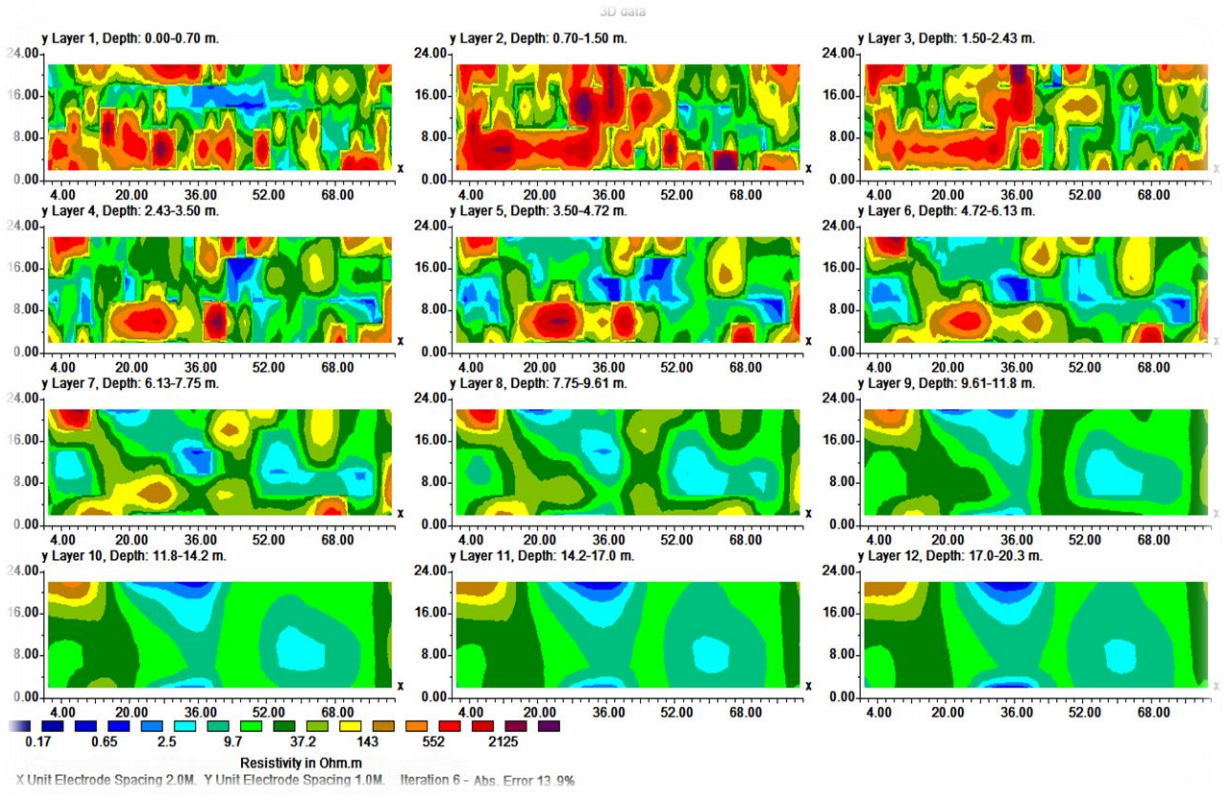

Fig 7. The inversion model for shallow unknown cavities shows 3-D resistivity distribution level slices for different depths using the robust constrain method

4. Conclusion

Both the 2-D and 3-D resistivity imaging models suggest a high number of caves in the studied area, especially in the upper section of the unconformity layer between the Anah and Euphrates formations. These caves have relatively high impedance resistivity values between 400 and 500 ohm.m. The study area is characterized by the presence of some small caves scattered near the surface of the earth. Therefore, the study area has greater risks to buildings. The horizontal slices of the 3-D models give a clear view of the subsurface image. It also reveals the presence of many small caves near the surface. 2D and 3D resistivity imaging values have large RMS errors for the inverted models, this confirms that the study area has high inhomogeneity. In addition to the broad spread of caves near the surface, this heterogeneity is created by a substantial difference in the resistivity of the rocks surrounding the caves. These findings suggest that the location poses a risk to the buildings that have been built there or those are expected to be built there in the future.

References

Abed AM (2013) Comparison between 2D imaging survey and traditional electrode arrays in delineating subsurface cavities in Haditha-Hit area (W. Iraq), Ph. D. Thesis (Unpublished), University of Baghdad, College of Science 7(3):166-75

Abed AM, Al-Zubedi AS, and Abdulrazzaq ZT (2020) Detected of gypsum soil layer by using 2d and 3d electrical resistivity imaging techniques in University of Anbar, Iraq, *Iraqi Geological Journal* 53 (2C):134-144.

Abed AM, Thabit JM, AL-Menshed FH (2021) An Attempt to Image Um El-Adam Cavity Structure in the Karst Terrain at Hit Area, *Western Iraq, Iraqi Geological Journal* 54 (1A), 44-54.

Al-Ane JM (1993) Detection subsurface cavities by using the electrical resistivity method in Hamam A-Alel area. *Journal of the Geological Society Iraq 26:13*–26,

Al-Hetty SO, Al-jibouri AS, Abed AM (2021) Description of the Karst Phenomena Spreading Along Stratified Sequence in the Western Desert of Iraq, *Iraqi Geological Journal* 54 (1B), 94-101.

Al-Zoubi AS, Abueladas AE, Al-Rzouq RI, Camerlynck C, Akkawi E, Ezarsky M, Abu-Hamattch ZSH, Ali W, Al Rawashdeh S (2007) Use of 2D multi electrodes resistivity imaging for sinkholes hazard assessment along the Eastern part of the Dead Sea, *Jordan. American Journal of Environmental Sciences* 3:230–234.

Aizebeokhai AP, Oyeyemi KD (2014) Application of geoelectrical resistivity imaging and VLF-EM for subsurface characterization in a sedimentary terrain,

Southwestern Nigeria. *Arabian Journal of Geosciences*8: 4083-4099.

Bentley LR, Gharibi M (2004) Two- and three-dimensional electrical resistivity imaging at a heterogeneous remediation site. Geophysics 69:674–680.

Busby JP (2000) The effectiveness of azimuthal apparent resistivity measurements as a method for determining fracture strike orientations. *Geophysical Prospecting* 48:677–695.

Chambers JE, Kuras O, Meldrum PI, Ogilvy RD, Hollands J (2006) Electrical resistivity tomography applied to geologic, hydrogeologic, and engineering investigations at a former waste-disposal site. Geophysics 71(6): B231–B239.

Chambers JE, Wilkinson PB, Wardrop D, Hameed A, Hill I, Jeffrey C, Loke, MH, Meldrum PI, Kuras O, Cave M, Gunn DA (2012) Bedrock detection beneath river terrace deposits using three-dimensional electrical resistivity tomography. Geomorphology 177–178:17–2520.

Dahlin T, Loke MH (1997) Quasi-3D resistivity imaging: mapping of 3D structures using two-dimensional dc resistivity techniques, 3rd Mtg., Environ. Eng. Geophysics. Assn., Expanded Abstracts, pp 143–146.

Dahlin T, Bernstone C, Loke MH (2002) A 3-D resistivity investigation of a contaminated site at Lernacken, Sweden. Geophysics 67(6):1692–1700.

Dutta NP, Rose RN, Saikia BC (1970) Detection of solution channels in limestone by electrical resistivity method. Geophysical Prospecting 28: 405–407.

Elawadi E, El-Qady G, Salem A, and Ushijma (2001) Detection of cavities using pole-dipole resistivity technique. Memoirs of the Facility of Engineering, Kyushu University 61(4):101-112.

Loke MH, Dahlin T (2010) Methods to reduce banding effects in 3-D resistivity inversion. In: Proceedings of the 16th *European Meeting of Environmental and Engineering Geophysics*, 6–8 Sep 2010, Zurich, Switzerland, A16.

Loke MH, Barker RD (1996) Practical techniques for 3D resistivity surveys and data inversion. Geophysical Prospecting 44:499–524.

Loke MH (2020) Tutorial: 2-D and 3D Electrical Imaging Surveys, Malaysia. http://www.geotomosoft.com/

Massoud U, Qady G, Metwaly, Santos F (2009) Delineation of a shallow subsurface structure by azimuthal resistivity sounding and joint inversion of VES-TEM data: case study near lake Qaroun, El Fayoum, Egypt. *Pure and applied geophysics* 166:701–719.

McDowell PW (1979) Geophysical mapping of water-filled fracture zones in rocks. International Association of Engineering Geology 19:258–264.

Obiadi II, Onwuemesi AG, Anike OL, Obiadi CM, Ajaegwu NE, Anakwuba EK, Akpunonu EO, Ezim EO (2012) Imaging subsurface fracture characteristics using 2D electrical resistivity tomography. *International Journal of Engineering Science* 1:103–110.

Rucker DF, Levitt MT, Greenwood WJ (2009) Three-dimensional electrical resistivity model of a nuclear waste disposal site. *Journal of Applied Geophysics* 69(3-4): 150–164.

Salman AM, Abed AM, Thabit JM (2020a) Comparison between Dipole-dipole and Pole-dipole arrays delineation of Subsurface Weak Zones Using 2D ElectricalImaging Technique in Al-AnbarUniversity, *Western Iraq, Iraqi Journal of Science* 61 (3): 567-576.

Salman AM, Thabit JM, Abed AM (2020b) Application of the Electrical Resistivity Method for Site Investigation in the University of Anbar, Ar-Ramadi City, *Western Iraq, Iraqi Journal of Science* 61(6): 1345-1352.

Sissakian V, Salih SM (1994) The Geology of Ramadi, Area. Map-NA- 38-9 (GM-18) Scale 125000, GEOSURV. UnpublishedInternal Report.

Sissakian V, Ibrahim E, Ibrahimand F, AL-Ali N (2005) Explanatory of Geological Hazard Map of Iraq 1st Edition, (Scale 1:1000000) D. Geol. Surv. (GEOSURV) Min. Invest, Baghdad.

White RMS, Collins S, Denne R, Hee R, Brown P (2001) A new survey design for 3D IP modeling at Copper hill. *Exploration Geophysics* 32(4):152–155.

Yang X, Lagmanson N (2006) Comparison of 2D and 3D electrical resistivity imaging methods. Symposium on the Application of Geophysics to *Engineering and Environmental Problems Proceedings*: 585–594.

Yilmaz S (2011) A case study of the application of electric resistivity imaging for investigation of a landslide at the highway. *International Journal of Physical Sciences* 6:5843–5849.